P H Y S I C A L   R E V I E W   L E T T E R S

Nucleation of Breathers via Stochastic Resonance in Nonlinear Lattices

David Cubero,[1] Jesús Cuevas,[1] and P. G. Kevrekidis[2]

[1]*Departamento de Física Aplicada I, EUP, Universidad de Sevilla, Calle Virgen de África 7, 41011 Sevilla, Spain*
[2]*Department of Mathematics and Statistics, University of Massachusetts, Amherst, Massachusetts 01003-4515, USA*

By applying a staggered driving force in a prototypical discrete model with a quartic nonlinearity, we demonstrate the spontaneous formation and destruction of discrete breathers with a selected frequency due to thermal fluctuations. The phenomenon exhibits the striking features of stochastic resonance: a non-monotonic behavior as noise is increased and breather generation under subthreshold conditions. The corresponding peak is associated with a matching between the external driving frequency and the breather frequency at the average energy given by ambient temperature.

PACS numbers: 63.20.Pw, 05.40.−a, 05.45.Xt, 05.45.Yv

Intrinsic localized modes, often referred to as discrete breathers, have been the focus of a number of theoretical studies (for a recent review see, e.g., [1]). One of the main reasons for the intense interest in these modes is the fact that they provide a natural setup for energy localization, a paradigm of interest to many areas of physics as well as chemistry and biology. Such discrete breathers have been rigorously proven to exist as time-periodic localized excitations in nonlinear Hamiltonian lattices [2]. Ever since, they have been experimentally observed in a wide variety of different media, ranging from optical waveguides and photorefractive crystals to micromechanical cantilever arrays and Josephson junctions, as well as in Bose-Einstein condensates and layered antiferromagnets [1,3].

In this Letter, having in mind realistic physical systems, we will focus on the nucleation of such breathers in a prototypical model system in which friction and ambient noise are also present. This will lead us to the consideration of stochastic resonance (SR), the counterintuitive phenomenon by which an appropriate dose of noise, instead of degradation, produces an enhancement of sensitivity of a nonlinear system to external forcing [4]. In spatially extended systems, SR has been shown for bistable [5] or excitable media [6], usually associated with pattern formation [7]; see, e.g., the review of [4].

Our prototypical nonlinear model will consist of a quartic potential (the so-called hard ϕ^4 lattice [8]) with the following equation of motion for each oscillator x_n ($n = 1, \ldots, N$) with mass m:

$$m\ddot{x}_n = -U'(x_n) + k(x_{n+1} + x_{n-1} - 2x_n)$$
$$- \alpha\dot{x}_n + \xi_n + F_n(t), \qquad (1)$$

where the overdot and the prime denote the time and space derivative, respectively; k is the coupling parameter between oscillators; α is the damping constant; $F_n(t)$ denotes external driving; and ξ_n is a Gaussian white noise with zero mean and autocorrelation $\langle \xi_n(t)\xi_m(t')\rangle = 2D\delta_{nm}\delta(t - t')$. The noise strength parameter D obeys the fluctuation-dissipation relation $k_B T = D/\alpha$, where k_B is the

Boltzmann constant and T the ambient temperature. Thus, D is an indicator of the level of noise associated with thermal fluctuations.

The on-site potential is given by $U(x) = ax^2/2 + bx^4/4$ with $a, b > 0$. Because of the monostable character of this potential, the noiseless lattice has a single stable steady state, allowing us to focus on the behavior of homoclinic orbits, rather than kinklike heteroclinic orbits, like in the bistable ϕ^4 case ($a < 0$). This is one way in which our work differs from the standard bistable models of SR, or the interesting recent work of [9], which considers noise-induced transitions between steady states in very short Fermi-Pasta-Ulam type, boundary-driven chains. Moreover, this model possesses a phonon band which can be easily determined upon linearization of (1) as $\omega_{\rm ph} \in (\sqrt{U''(0)/m}, \sqrt{[U''(0) + 4k]/m})$ [1]. Thus, by exciting breathers with a frequency larger than the maximum frequency of the phonon spectrum, $\omega_{\rm max} = \sqrt{(a + 4k)/m}$, these localized modes are guaranteed not to interact with the phonons, avoiding effects like radiation resonances which slowly dissipate away the energy of discrete breathers [10].

Indeed, the associated Hamiltonian system of this hard model [i.e., Eq. (1) without damping and noise] exhibits exponentially localized in space and periodic in time high (i.e., higher than $\omega_{\rm max}$) frequency excitations. An example is the dynamically stable Sievers-Takeno (ST) [11] site-centered mode. As shown in Fig. 1, this mode is staggered; i.e., the neighboring sites oscillate out of phase. Hence, these breathers will necessitate that we impose staggered periodic driving in order to sustain them in the presence of dissipation. For this reason, we shall consider the following ac driving force:

$$F_n(t) = (-1)^n F_0 \sin(\Omega t). \qquad (2)$$

Its effect on a deterministic Fermi-Pasta-Ulam lattice has been studied in Ref. [12].

Equation (1) is supplemented with (periodic) boundary conditions $x_0 = x_N$ and $x_{N+1} = x_1$. Generally, ϕ^4 models have been commonly used to describe a wide range of
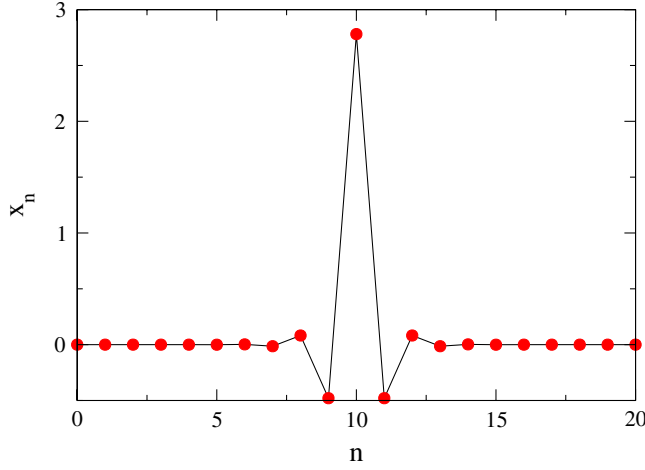
205505-1

FIG. 1 (color online). Spatial profile of a staggered high-frequency ($\omega = 3$) Hamiltonian breather generated using methods based on the anticontinuous limit [21]. The line is a guide to the eye.

phenomena from elementary particle collisions and cosmological domain walls [13] to droplet nucleation and phase transitions [14], constituting a prototypical nonlinear model in statistical field theory [15].

For the sake of a dimensionless description, we can scale all lengths and times by the characteristic length $\lambda = (a/b)^{1/2}$ and time $\tau = (m/a)^{1/2}$, i.e. $\tilde{x}_n = x_n/\lambda$, $\tilde{t} = t/\tau$, which implies $\tilde{k} = k/a$, $\tilde{\alpha} = \alpha/(am)^{1/2}$, $\tilde{D} = bD/(a^5m)^{1/2}$, and $\tilde{F}_0 = F_0(b/a^3)^{1/2}$. In the following we will omit the tilde symbols for simplicity. The dimensionless form of the equations of motion (1) then reads

$$\ddot{x}_n = -x_n - x_n^3 + k(x_{n+1} + x_{n-1} - 2x_n)$$
$$- \alpha\dot{x}_n + \xi_n + (-1)^n F_0 \sin(\Omega t). \quad (3)$$

Let us discuss, for the moment, the deterministic behavior of (3) (i.e., without noise, $D = 0$). As mentioned above, the staggering factor $(-1)^n$ in (2) is important in order to sustain the breathers in the presence of dissipation. When that factor is absent, the ST breather shown in Fig. 1 is always observed to die out, regardless of the driving strength. However, in addition to this staggering factor, the driving amplitude F_0 must be large enough so that the energy supplied by the driving force is able to compensate for the energy which has been dissipated by the friction force. Breathers in the dissipative deterministic lattice can be calculated using a method similar to that developed in [16]. An analysis of those breathers shows that, for $k = 1$ and $\alpha = 0.1$ and a breather frequency of $\omega = \Omega = 3$, there is a threshold at $F_{th} = 0.6092$. When the driving amplitude is below this threshold (subthreshold amplitude), the dissipation gradually drains away the system's energy, and breather modes cannot be supported. In the following, unless explicitly stated, we will assume $k = 1$, $\alpha = 0.1$, and $\Omega = 3$, which implies $\omega_{max} = \sqrt{5} < \Omega$.

Having summarized the results of the deterministic case, let us now turn to the analysis of the effect of thermal fluctuations and how they modify this picture. Starting with the suprathreshold case ($F_0 > F_{th}$), we would expect that the addition of noise provokes the spontaneous formation of breathers with the frequency dictated by the external driving, even if the system starts from a uniform configuration. This is indeed what is observed, as shown in Fig. 2, where a typical realization of the oscillators' trajectories has been plotted. The frequencies and amplitudes of the observed noise-induced breathers are very similar to the deterministic ST breather depicted in Fig. 1. The ST breather has the smallest size and the lowest energy of all possible collective modes at the frequency of the driver, thus being the most probable breather to be induced by noise. However, unlike the deterministic case, the breathers are not permanent, and the same random force which has generated them is able to destroy them after a while.

In the subthreshold case the driving force is not able by itself to sustain the breathers. Remarkably, however, the simulations show that these breathers are still produced in the system by the concerted action of noise and the driving force. This is shown in Fig. 3. The bottom panel shows a comparison of one of these noise-induced breathers with the deterministic stable breather obtained with a suprathreshold driving force. This effect resembles one of the main features of the earliest manifestations of SR: the noise-induced hopping events of a Brownian particle in a bistable potential subject to a externally applied force which taken alone is not sufficient to produce the hopping events [4]. Noise appears then as beneficial, enabling system transitions between the uniform background state and the coherent, localized breather patterns. On the other
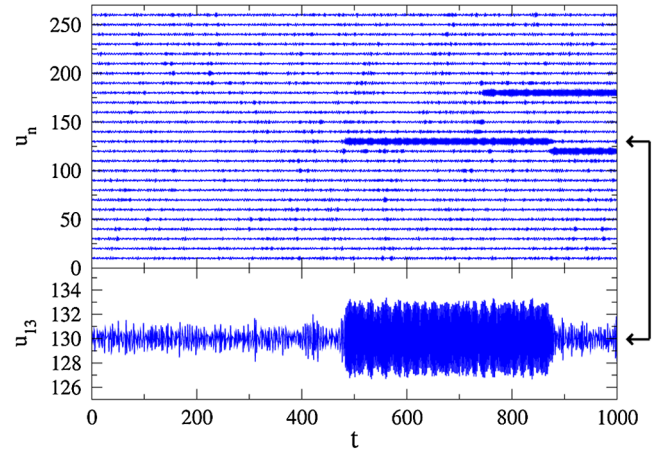

FIG. 2 (color online). Time evolution of the oscillator positions $u_n(t) := x_n(t) + 10n$ for a system subject to a suprathreshold driving with $F_0 = 1$ and $\Omega = 3$, and noise strength $D = 0.1$ starting from a uniform initial condition $x_n(0) = 0$. Breathers are observed to form and vanish spontaneously. The bottom panel shows a magnification of the time evolution of an oscillator which becomes the center of a high-frequency breather.
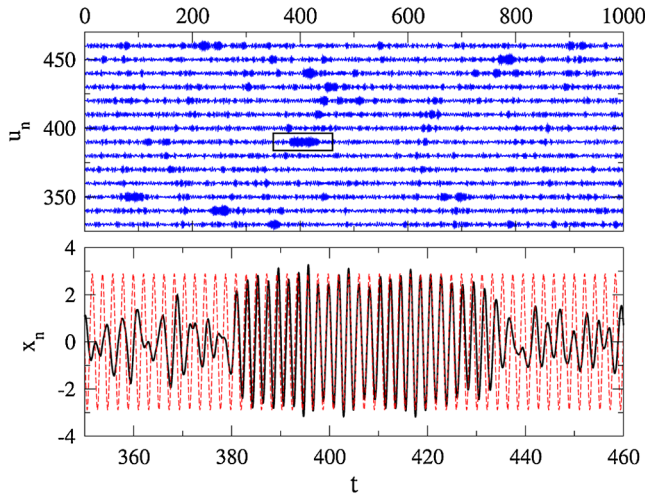
FIG. 3 (color online). Same as in Fig. 2 but for a subthreshold amplitude $F_0 = 0.6$ and noise strength $D = 0.3$. The bottom panel shows a magnification of part of the trajectory $x_n(t)$ of one oscillator (boxed in the upper panel), as well as the time evolution of the center oscillator of a deterministic ($D = 0$) and dissipative breather ($\alpha = 0.1$) with suprathreshold $F_0 = 1$ and same driving frequency (dashed red line).

hand, we would expect that if the thermal fluctuations are very large, they will destroy any degree of order in the system, producing the nonmonotonic behavior characteristic of the SR phenomenon. This scenario should offer a generic mechanism for the formation of breatherlike excitations in realistic nonlinear lattices where fluctuations are present.

In order to quantify these effects, we have computed numerically the Fourier coefficient of an arbitrary oscillator at the frequency of the external driver,

$$q = \frac{2}{T} \int_0^{2\pi/\Omega} dt\, e^{-i\Omega t} \langle x_1(t) \rangle_\infty, \tag{4}$$

where the notation $\langle \ldots \rangle$ indicates an average over noise realizations and the subindex ∞ indicates the long time limit of the noise average, i.e., its value after waiting a long enough time for the transients to die out. Every time the oscillator x_1 is part of a breather, or a collective attempt to form a breather mode at the frequency of the driver, will result in a larger coefficient q. The choice of the oscillator in (4) is irrelevant because of the periodic boundary conditions. The simulations were performed with $N = 40$ and $N = 60$ oscillators, the larger value carried out in order to check that the results did not depend on the system size.

We present in Fig. 4 the values of the amplitude $|q|^2$ as a function of the noise strength D for a suprathreshold and subthreshold driving. The nonmonotonic behavior with noise, a recognized signature of the SR phenomenon, is very clear in both the suprathreshold and subthreshold situations. Nevertheless, let us note that a nonmonotonic behavior is also obtained when we inhibit breather formation by canceling the interaction between the oscillators. The dotted line in Fig. 4 shows this feature for a system
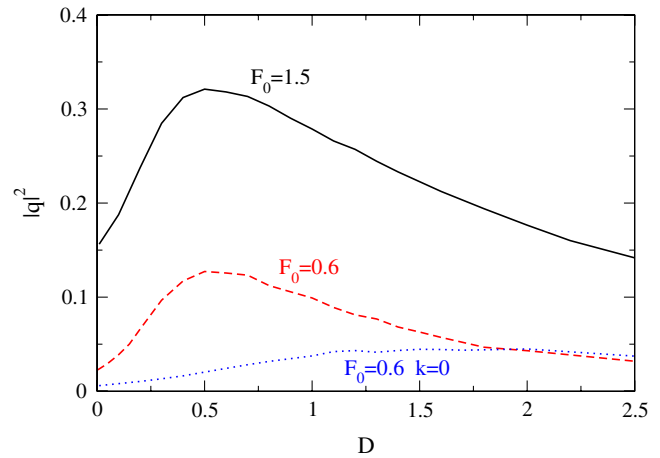

FIG. 4 (color online). The Fourier amplitude $|q|^2$, defined in Eq. (4), as a function of the noise strength D for a suprathreshold driving $F_0 = 1.5$ (solid line), a subthreshold driving $F_0 = 0.6$ (dashed line), and a system with $F_0 = 0.6$ but without interaction between the oscillators, i.e. $k = 0$ (dotted line).

with $k = 0$. This is a well-known phenomenon for any single-oscillator system subject to a nonlinear monostable potential, both in the underdamped [17] or overdamped [18] regime. In the former, the peak is produced by a matching between the driving frequency and the intrinsic frequency associated with the most probable excitation energy, which is a monotonic function of the noise strength [17]. In fact, a simple classical mechanics analysis of the undriven Hamiltonian system (α, D, $F_0 = 0$) with $k = 0$ shows that a periodic solution with frequency $\omega = 3$ corresponds to an energy per particle value of $E/N = 36$. Under thermal equilibrium ($F_0 = 0$), we need to raise the temperature to a value such that the noise strength is $D = 1.67$ in order to obtain an average energy per particle of the same value. It can be seen in Fig. 4 that this value of D is in good agreement with the position of the maximum. A similar argument also holds when we switch on the interaction between the oscillators, though now collective excitations associated with lower energies are allowed, resulting in larger amplitudes with a peak at a lower value of D. The total energy associated with the breather presented in Fig. 1 is $E = 30$. If we consider that roughly only $l = 5$ oscillators are needed to form the ST breather, an average energy per particle of $E/N = 6$ would be necessary in order to optimize breather formation. This value is obtained at thermal equilibrium when $D = 0.7$, which is a reasonable estimation of the peak position observed in Fig. 4. A better estimation, namely, a peak at $D = 0.47$, is obtained if we choose $l = 7$ oscillators. The appropriate value of l is determined by the correlation length, as discussed below.

For an arbitrarily small driving amplitude F_0, linear response theory [19,20] predicts

$$\langle x_1(t) \rangle_\infty = \int_0^\infty ds\, \chi(s) f(t - s), \tag{5}$$
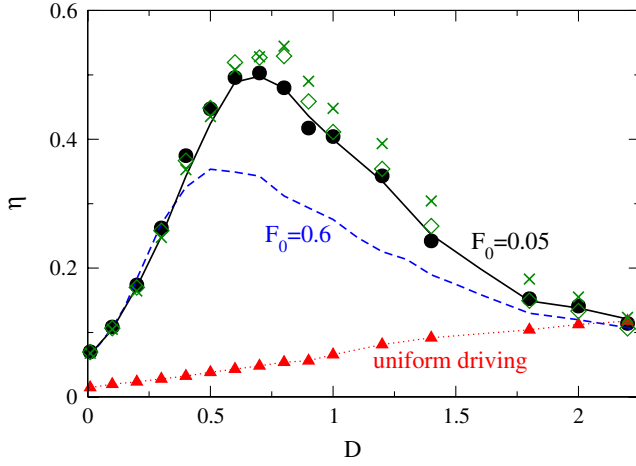
FIG. 5 (color online). Spectral amplification $\eta = |q|^2/F_0^2$ as a function of noise. Filled circles depict the linear response results, computed numerically using Eq. (7), and the solid line the simulation results for $F_0 = 0.05$. The dashed line corresponds to $F_0 = 0.6$. Crosses and diamonds correspond to a linear response calculation neglecting correlations between oscillators separated by more than 2 and 3 sites, respectively. Filled triangles depict the linear response prediction for a system with a uniform external driving $F_n(t) = F_0 \sin(\Omega t)$ (for all n) instead of (2). The dotted line is a guide to the eye.

where $f(t) = F_0 \sin(\Omega t)$ and $\chi(t)$ is the response function. This function can be expressed in terms of equilibrium time correlation functions,

$$\chi(t) = -\frac{\alpha}{D}\frac{d}{dt}\langle x_1(t)M(0)\rangle_{\text{eq}}, \qquad (6)$$

where $\langle\ldots\rangle_{\text{eq}}$ denotes equilibrium averages in the absence of driving and $M(t) = \sum_{n=1}^{N}(-1)^n x_n(t)$ is part of the perturbing Hamiltonian $-Mf(t)$ associated with the external driving. The calculation of the Fourier coefficient of (5), together with the definitions $\chi_r = \int_0^\infty \chi(t)\cos(\Omega t)$ and $\chi_i = \int_0^\infty \chi(t)\sin(\Omega t)$, yields the following spectral amplification $\eta = |q|^2/F_0^2$:

$$\eta = [\chi(0) - \chi_i\Omega]^2 + (\chi_r\Omega)^2. \qquad (7)$$

Figure 5 shows the linear response results obtained from simulations at thermal equilibrium. It is seen that a driving amplitude of $F_0 = 0.05$ is small enough to be within linear response theory. Because of the presence of noise and dissipation, the correlation between two separated oscillators decreases rapidly as their separation is increased. In fact, Fig. 5 shows that a good approximation is obtained if the time correlation functions $\langle x_1(t)x_n(0)\rangle_{\text{eq}}$ corresponding to oscillators separated by more than 2 sites ($|n-1| > 2$) are neglected in Eq. (6). This is consistent with the above energy matching argument with $l = 5$, and the dynamical role of ST breathers, leading to the peak estimation at $D = 0.7$. Larger driving amplitudes are associated with larger correlation lengths, producing a peak at slightly lower values of D.

Finally, the calculated correlation functions allow us to readily compute the system response when the driving force acting on each oscillator is not staggered but spatially uniform, i.e., $M(t) = \sum_{n=1}^{N} x_n(t)$. The dotted line in Fig. 5 shows that the spectral amplification is very similar to that when breather formation was strictly forbidden (the case $k = 0$ shown in Fig. 4), lacking the stronger peak at lower noise levels. As expected from the deterministic analysis, this uniform driving force is very ineffective in boosting breather formation.

In conclusion, we have demonstrated the spontaneous formation of breathers in a hard ϕ^4 lattice subject to a staggered driving force. The formation of noise-induced breathers with the selected driving frequency is optimized for a given level of fluctuations such that the average energy per particle matches the intrinsic energy of the breather mode. We expect these results to be useful for the generation and manipulation of breathers, and to be independent of dimension and of the specific nature of the nonlinearity, provided that the model is monostable.

[1] S. Flach and A. Gorbach, Phys. Rep. **467**, 1 (2008).
[2] R. MacKay and S. Aubry, Nonlinearity **7**, 1623 (1994).
[3] D. K. Campbell, S. Flach, and Yu. S. Kivshar, Phys. Today **57**, No. 1, 43 (2004).
[4] L. Gammaitoni et al., Rev. Mod. Phys. **70**, 223 (1998).
[5] F. Marchesoni, L. Gammaitoni, and A. R. Bulsara, Phys. Rev. Lett. **76**, 2609 (1996).
[6] P. Jung and G. Mayer-Kress, Phys. Rev. Lett. **74**, 2130 (1995).
[7] J. Vilar and J. M. Rubí, Phys. Rev. Lett. **78**, 2886 (1997).
[8] D. Chen, S. Aubry, and G. P. Tsironis, Phys. Rev. Lett. **77**, 4776 (1996).
[9] G. Miloshevich et al., Phys. Rev. Lett. **102**, 020602 (2009).
[10] M. Johansson and S. Aubry, Phys. Rev. E **61**, 5864 (2000).
[11] A. J. Sievers and S. Takeno, Phys. Rev. Lett. **61**, 970 (1988).
[12] R. Khomeriki, S. Lepri, and S. Ruffo, Phys. Rev. E **64**, 056606 (2001); Physica (Amsterdam) **168–169D**, 152 (2002).
[13] P. Anninos et al., Phys. Rev. D **44**, 1147 (1991).
[14] J. S. Langer, Ann. Phys. (Leipzig) **41**, 108 (1967).
[15] G. Parisi, Statistical Field Theory (Perseus Books, New York, 1998).
[16] J. L. Marín et al., Phys. Rev. E **63**, 066603 (2001).
[17] N. G. Stocks et al., J. Phys. A **26**, L385 (1993).
[18] M. Evstigneev et al., Europhys. Lett. **65**, 7 (2004).
[19] P. Hänggi and H. Thomas, Phys. Rep. **88**, 207 (1982).
[20] R. Zwanzig, Nonequilibrium Statistical Mechanics (Oxford University Press, New York, 2001).
[21] J. L. Marín and S. Aubry, Nonlinearity **9**, 1501 (1996).